Band-Structure-Dependent Demagnetization in the Heusler Alloy $Co_2Mn_{1-x}Fe_xSi$

Daniel Steil,[1] Sabine Alebrand,[1] Tobias Roth,[1] Michael Krauß,[1] Takahide Kubota,[2] Mikihiko Oogane,[2] Yasuo Ando,[2] Hans Christian Schneider,[1] Martin Aeschlimann,[1] and Mirko Cinchetti[1]

[1]*Department of Physics and Research Center OPTIMAS, University of Kaiserslautern, 67653 Kaiserslautern, Germany*
[2]*Department of Applied Physics, Graduate School of Engineering, Tohoku University, Sendai 980-8579, Japan*

(Received 9 June 2010; published 15 November 2010)

We investigate the ultrafast demagnetization for two Heusler alloys ($Co_2Mn_{1-x}Fe_xSi$) with a different lineup of the minority band gap and the Fermi level. Even though electronic spin-flip transitions are partially blocked by the band gap in one compound, the respective magnetization dynamics, as measured by the time-resolved Kerr effect, are remarkably similar. Based on a dynamical model that includes momentum and spin-dependent carrier scattering, we show that the magnetization dynamics are dominated by *hole* spin-flip processes, which are not influenced by the gap.

DOI: 10.1103/PhysRevLett.105.217202 PACS numbers: 75.78.Jp, 71.20.Be, 75.70.−i

Starting with pioneering experiments on ferromagnetic nickel [1] in 1996, the field of ultrafast magnetization dynamics has seen a constant development of experimental [2–5] and theoretical studies [6–8]. It is now an experimentally well established fact that the 3*d* ferromagnets Fe, Ni, and Co show characteristic demagnetization times on the order of some 100 fs after optical excitation. On the theoretical side, several models based on Elliott-Yafet–type spin-dependent scattering have been proposed [6,9–11] to explain the available experimental data. The point of view introduced and analyzed in Ref. [9] is that the demagnetization results from multiband nonequilibrium carrier dynamics due to momentum-dependent electron-electron scattering in the presence of the spin-orbit interaction. This picture is close to the one used to explain ultrafast spin relaxation of holes due to the strong spin-orbit interaction in the hole bands of bulk GaAs [12]. By adapting this model for the ferromagnetic metals cobalt and nickel by incorporating an approximate band structure, a good agreement with magneto-optical Kerr effect measurements was obtained for the ultrafast magnetization dynamics.

The band structure determines the possible transitions between states of different momenta in a typical scattering process (together with the relevant matrix elements), regardless whether such a transition, $\vec{k} \rightarrow \vec{k} + \vec{q}$, say, is due to carrier-carrier, carrier-phonon, or carrier-impurity interactions. Here we investigate half-metallic Heusler alloys that possess a band gap in one spin channel at the Fermi level E_F. A band gap in one spin channel, as realized in the density of states of Heusler alloys schematically shown in Fig. 1, suggests that the demagnetization dynamics after optical excitation is fundamentally different from that in 3*d* ferromagnets: For instance, the presence of a gap above E_F for minority-spin carriers blocks electronic transitions of optically excited electrons from majority-spin ($\uparrow$) to minority-spin ($\downarrow$) states close to the Fermi level because of a lack of empty final states. This electronic *minority-state blocking* [13–15] seems to imply that energy and angular momentum transfer between the two spin channels should take place considerably more slowly than in a comparable system without a gap. In particular, the demagnetization should not be ultrafast, as in the case of ferromagnetic metals, but should occur on time scales on the order of a few hundred picoseconds. However, such a slow demagnetization is not observed experimentally for all half-metals [13].

In this Letter, we provide a microscopic picture of the carrier dynamics underlying the demagnetization in two half-metallic Heusler alloys, whose band lineups are chosen such that only one of them should show minority-state blocking but which are also sufficiently similar to allow comparison between them. Heusler alloys exhibit the composition formula X_2YZ, where X and Y are transition metals and Z is a main group element. Some of their properties are similar to the underlying transition metals. A well-known method to tailor their band structure consists in substituting the transition metal Y or the element Z in

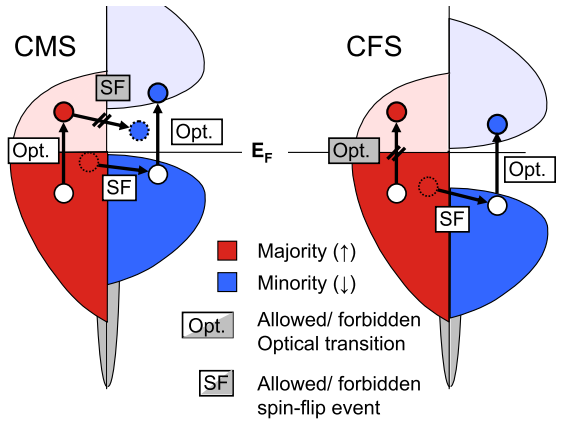

FIG. 1 (color online). Schematic density of states for the Heusler alloys CMS and CFS. Note that the band gap is above E_F for CMS and below E_F for CFS [17]. Transitions induced by the optical pump pulse and spin-flip scattering pathways are also shown.

quaternary compounds [16]. For the substitutional quaternary Heusler compound $Co_2Mn_{1-x}Fe_xSi$, band structure calculations [17] have shown half-metallic properties and a Fermi energy that moves in the minority band gap from the top of the valence band to the bottom of the conduction band when the concentration x is increased. For $x = 0$, i.e., Co_2MnSi or CMS for short, the Fermi energy is lined up to the top of the valence band; for $x = 1$, i.e., Co_2FeSi, or CFS for short, the Fermi energy is lined up to the bottom of the conduction band; see Fig. 1. CMS should exhibit minority-state blocking, whereas in CFS the band gap is mainly in the occupied part of the minority channel, so that spin-flip transitions from the majority to the minority channel above E_F are, in principle, allowed. However, the lineup of the band gap, which determines the availability of final minority states for spin-flip transitions from majority bands, is not the only deciding factor for the efficiency of the demagnetization by spin-flip transitions after optical excitation. Using model calculations we show that one also needs to take into account the efficiency of the optical excitation for majority and minority bands, as well as the carrier dynamics in bands below the Fermi energy. The latter contribution to the demagnetization dynamics becomes possible because holes, i.e., empty states below the Fermi energy, are created by optical pump fields. This turns out to be the relevant mechanism leading to ultrafast demagnetization in the investigated samples.

Experiments were performed by using a time-resolved magneto-optical Kerr effect (TR-MOKE) setup utilizing an 800 nm, 1 kHz fs-amplifier system with a pulse duration of ≈ 50 fs at the sample position [2,9,11]. The pump fluence was 4.5 mJ/cm^2. All data were recorded in the polar Kerr geometry by using a dichroic pump-probe setup. The Kerr rotation is detected by using a balanced-bridge detector and a lock-in amplifier. An active beam stabilization and a double sample holder were used to ensure a consistent pump-probe overlap on the two samples. The pump spot is over 1 order of magnitude larger than the probe spot, so that the material response is probed in a homogeneously excited area. The epitaxial CFS and CMS samples were 30 nm thick films capped by 2 nm tantalum with a 40 nm chromium buffer layer on a MgO(001) substrate. For details on sample properties, see [18].

Figure 2 shows the TR-MOKE results for demagnetization of the CFS and CMS samples excited by the same pump fluence. Using a least-squares exponential fit of the form $A\exp[-(t - t_0)/\tau_M]$ yields time constants of $\tau_M = 198^{-39}_{+64}$ fs for CFS and $\tau_M = 265^{-32}_{+42}$ fs for CMS, in agreement with recent measurements on CMS [13,19] performed with the same pump wavelength. The maximum relative quenching of the magnetization is $72 \pm 1.5\%$ vs $64 \pm 1.3\%$, respectively. The magnetization dynamics is quite fast for both samples, which is puzzling for different reasons: First, CMS exhibits minority-state blocking that should lead to a much slower demagnetization than observed.

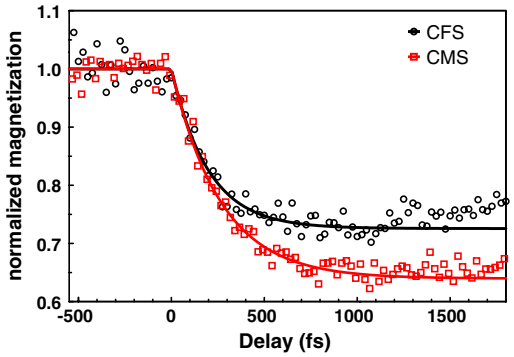

FIG. 2 (color online). Magnetization dynamics of CFS (black circles) and CMS (red squares) measured by TR-MOKE with a pump fluence of 4.5 mJ/cm^2. Lines are exponential fits (see text).

One explanation given in Ref. [13] is that defect states [20,21] may provide additional spin-flip channels in the band gap of CMS. Second, although CFS does not exhibit minority-state blocking, a closer inspection of the band structure of CFS [see Fig. 3(a) or [17]] shows that for an 800 nm optical pump there is hardly any excitation of majority electrons because the occupied and unoccupied majority bands are always more than 2 eV apart. The lack of excited majority electrons makes an efficient conversion of majority to minority electrons via spin-flip scattering and a concomitant fast demagnetization very unlikely.

To understand the microscopic processes leading to the magnetization dynamics, we performed model calculations

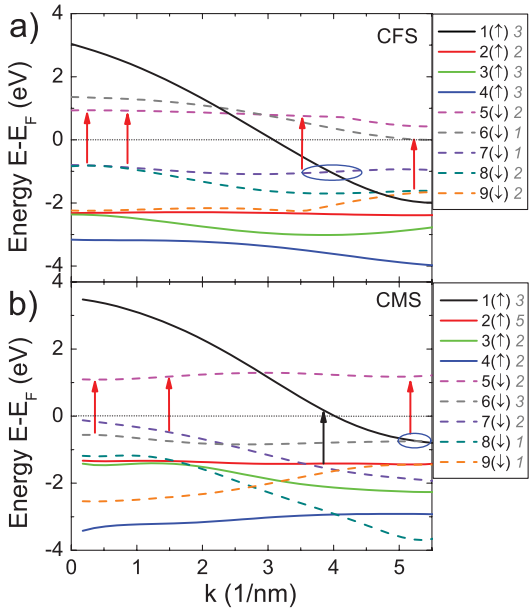

FIG. 3 (color). Majority (↑) and minority (↓) bands for (a) CFS and (b) CMS used for calculations. Optical transitions are shown as black (red) arrows for majority (minority) bands. Regions of dominant spin-flip transitions are marked by an ellipse. Degeneracies are included in gray italics in the legends.

for an Elliott-Yafet–type spin relaxation due to the interplay of electron-electron scattering and the spin-orbit interaction. The electronic dynamics is described by momentum-resolved electronic distribution functions in the bands of interest, and the interaction, which leads to the spin-relaxation dynamics, is taken into account at the level of momentum-resolved Boltzmann scattering integrals; see Ref. [9] for more details. The calculation uses as input the band structure in the whole Brillouin zone as well as an average spin mixing parameter $\alpha = 0.15$. The momentum dependence of the bands, which are shown in Fig. 3, is simplified by approximating them as spherically symmetric, i.e., by taking the band structure (from Ref. [17]) in the Γ-X direction to be same in all directions [22]. To reduce the numerical complexity, some bands have been treated as a single, degenerate band (cf. legend in Fig. 3). Despite these simplifications, the numerical treatment still captures essential properties of the momentum-resolved dynamics of the carrier distributions and allows one to determine the macroscopic magnetization dynamics from the microscopic carrier dynamics.

Figure 4 shows the results of the dynamical calculations for the momentum-integrated carrier densities in the different bands included in the calculations and the magnetization derived from these densities. From Fig. 4(a), we obtain a demagnetization time constant for CFS of $\tau_M^* = 321$ fs,

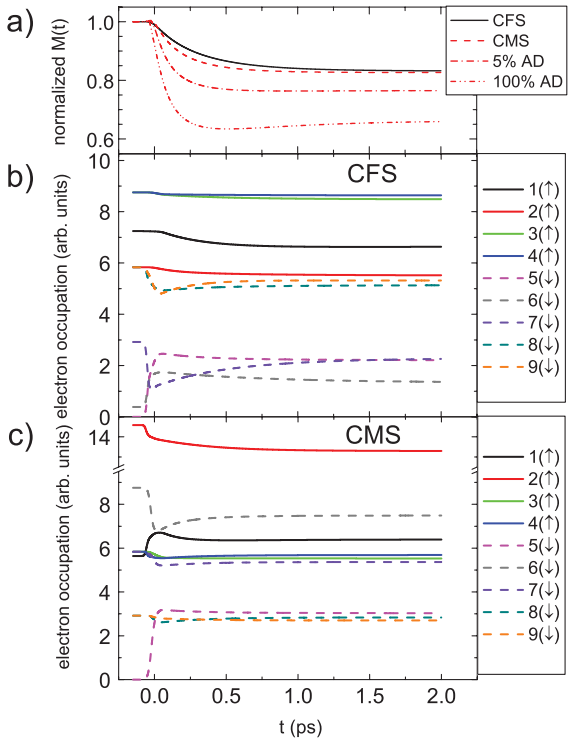

FIG. 4 (color). (a) Calculated transient magnetization for CFS and CMS including calculations for CMS with 5% and 100% Co AD. Electronic occupation of bands for (b) CFS and (c) CMS. Displayed is an effective occupation number density, which it not normalized, because it includes several, almost degenerate bands.

in good agreement with experiment. The changes in occupation of majority and minority bands underlying the magnetization dynamics in CFS are shown in Fig. 4(b). Because of the material band structure and the assumption that the optical excitation does not change the spin, no direct optical excitation into unoccupied majority-spin states is allowed. Indeed, no majority band is populated by the pump pulse. For the minority bands, optical transitions are possible from the 7(↓) and 8(↓) bands to both 5(↓) and 6(↓). Dominant transitions are marked in Fig. 3 by arrows. On longer time scales (hundreds of femtoseconds) a loss of electronic occupation is visible for *all* majority bands, especially for the 1(↑) band. In contrast, the optically populated minority 5(↓) and 6(↓) bands above E_F show only weak losses. Minority bands below E_F, especially 7(↓), are repopulated. Thus the demagnetization occurs mainly by effective spin-flip scattering between the majority 1(↑) band and the minority 7(↓) band, taking place below E_F for momenta ranging from 3.5 to 4.5 nm^{-1}. In this region, marked by an ellipse in Fig. 3(a), there is a high scattering rate for spin-flip transitions between the majority 1(↑) band and the minority 7(↓) band because the bands are energetically close around the crossing point. Moreover, around this point in the band structure, optical transitions in the minority channel are allowed, so that the optical pump field creates minority holes that provide the necessary phase space for the spin-flip scattering. The electrons in the minority bands above E_F do not significantly influence demagnetization dynamics, because the spin-flip scattering into the majority 1(↑) band is ineffective, as visible from the weak occupation losses of bands 5(↓) and 6(↓) in Fig. 4(b).

Figure 4(a) shows magnetization dynamics for CMS with a time constant of $\tau_M^* = 208$ fs, which is similar to the result for CFS. From the calculated carrier distributions for CMS in Fig. 4(c) and the band structure of Fig. 3, we find two major differences to CFS (schematically depicted in Fig. 1): (i) First, the 800 nm pump pulse excites not only minority [predominantly 6(↓) to 5(↓)] but also majority [2(↑) to 1(↑)] electrons from occupied to unoccupied states and thus creates transient holes below E_F. (ii) Second, above E_F spin-flip transitions are possible only for the minority electrons, as the band gap prohibits spin flips in the other direction, which is a signature of minority-state blocking [13]. Despite these differences, the magnetization dynamics is dominated by spin-flip scattering from the majority 1(↑) band into holes created in the minority 6(↓) band by the optical excitation [see ellipse in Fig. 3(b)]. All other bands play a less significant role. Since this kind of process is also the dominating one in CFS, a comparable magnetization dynamics is observed in the two compounds.

To illustrate the processes that underlie the dynamics of the momentum-integrated densities in CMS shown in Fig. 4(c), we plot in Fig. 5 the *momentum-resolved* carrier distribution of the majority band 1(↑): One notices the

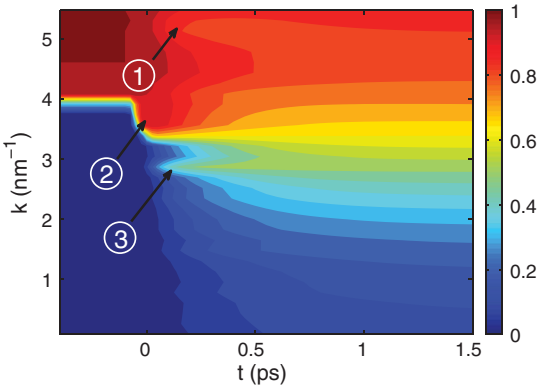

FIG. 5 (color). Momentum- and time-resolved occupation of the CMS majority band 1(↑). Relevant signatures of optical excitation and spin-flip scattering are marked by arrows.

signature of the optical excitation from the 2(↑) band below $k = 4$ nm^{-1}, marked with 2. There is also the loss of density due to outscattering processes [into the 6(↓) band] around $k = 5$ nm^{-1} (marked with 1) and a refilling into band 1(↑) around $k = 2.7$ nm^{-1} from the 5(↓) band (marked with 3). Figure 4(c) shows in comparison that the contribution of the minority electrons above E_F to the dynamics is almost negligible: A slight loss of carrier density on longer time scales is visible for the 5(↓) band.

From the discussion of the computed carrier dynamics underlying the demagnetization in CFS and CMS, it emerges that the demagnetization dynamics is not so much determined by the location of the gap, which may provide or block empty minority carrier states, but rather by the optical excitation and the momentum-resolved band structure, both above and below the Fermi level. Based on this model, the ultrafast demagnetization of CMS is not necessarily an indication of an imperfect half-metallicity of the compound as was argued in Ref. [13]. To further prove that defect states located in the band gap of CMS do not play the dominant role in the magnetization dynamics, we performed simulations including a dispersionless defect band −0.15 eV below the Fermi energy in the CMS band structure, similar to a defect band reported for Co antisite defects (AD) in [21]. The resulting $M(t)$ curve for two AD densities is shown in Fig. 4(a) together with the curve without defects. Even for the unrealistic assumption of 100% defect states, only a faster demagnetization by a factor of 2 is observed in comparison to the CMS without AD. Both times are 3 orders of magnitude away from the values found for CrO_2 in Ref. [13]. Thus, even by taking defect states into account, our conclusion remains valid.

In conclusion, we studied ultrafast demagnetization dynamics in the Heusler compounds CFS and CMS with TR-MOKE and compared the experimental results to microscopic calculations of the momentum-resolved carrier distributions in different bands. Comparable demagnetization times for CMS and CFS are found. We show that the demagnetization depends both on the excitation mechanism and on the details of the band structure, such as the existence of dispersive majority bands crossing E_F (prohibiting optical excitation in the majority channel) and flat minority bands in CFS. Our model calculations indicate that the demagnetization dynamics is dominated by spin-flip processes below the Fermi energy where the optical excitation has created holes which allow for transitions from majority bands to minority bands. We find that one cannot make qualitative predictions for the slow demagnetization dynamics based on minority-state blocking alone, especially when hole spin-flip transitions are important. Finally, our calculations indicate that the Heusler alloys under consideration even need not be perfect half-metals to show the observed demagnetization dynamics, because the band gap is not the decisive factor for the carrier dynamics underlying the demagnetization.

We gratefully acknowledge the DFG for funding within the GRK 792 and Research Units FG559 and ASPIMATT and the EC FP7 under Grant Agreement No. NMP3-SL-2008-214469 (UltraMagnetron).

[1] E. Beaurepaire *et al.*, Phys. Rev. Lett. **76**, 4250 (1996).
[2] M. Cinchetti *et al.*, Phys. Rev. Lett. **97**, 177201 (2006).
[3] E. Carpene *et al.*, Phys. Rev. B **78**, 174422 (2008).
[4] C. Stamm *et al.*, Nature Mater. **6**, 740 (2007).
[5] H.-S. Rhie, H. A. Dürr, and W. Eberhardt, Phys. Rev. Lett. **90**, 247201 (2003).
[6] B. Koopmans *et al.*, J. Magn. Magn. Mater. **286**, 271 (2005).
[7] G. P. Zhang and W. Hübner, Phys. Rev. Lett. **85**, 3025 (2000).
[8] D. Steiauf and M. Fähnle, Phys. Rev. B **79**, 140401 (2009).
[9] M. Krauß *et al.*, Phys. Rev. B **80**, 180407 (2009).
[10] D. Steiauf, C. Illg, and M. Fähnle, J. Magn. Magn. Mater. **322**, L5 (2010).
[11] B. Koopmans *et al.*, Nature Mater. **9**, 259 (2010).
[12] M. Krauß, M. Aeschlimann, and H. C. Schneider, Phys. Rev. Lett. **100**, 256601 (2008).
[13] G. M. Müller *et al.*, Nature Mater. **8**, 56 (2009).
[14] T. Kise *et al.*, Phys. Rev. Lett. **85**, 1986 (2000).
[15] Q. Zhang *et al.*, Phys. Rev. B **74**, 064414 (2006).
[16] P. Klaer *et al.*, Phys. Rev. B **80**, 144405 (2009).
[17] B. Balke *et al.*, Phys. Rev. B **74**, 104405 (2006).
[18] T. Kubota *et al.*, Appl. Phys. Lett. **94**, 122504 (2009).
[19] S. Mizukami *et al.*, J. Phys. Conf. Ser. **200**, 042017 (2010).
[20] S. Picozzi, A. Continenza, and A. J. Freeman, Phys. Rev. B **69**, 094423 (2004).
[21] S. Picozzi and A. J. Freeman, J. Phys. Condens. Matter **19**, 315215 (2007).
[22] According to the band structure calculations in Ref. [17], no optical excitation with 1.55 eV energy is possible for all other symmetry directions.